Acta Cryst. (1991). B47, 425–433

Space-Group Determination and Structure Model for κ-Al_2O_3 by Convergent-Beam Electron Diffraction (CBED)

BY PING LIU* AND JAN SKOGSMO

Department of Physics, Chalmers University of Technology, S-412 96 Göteborg, Sweden

(*Received* 13 *November* 1990; *accepted* 10 *January* 1991)

Abstract

The crystal structure of κ-Al_2O_3, which was produced by chemical vapour deposition, has been examined by convergent-beam electron diffraction combined with selected-area electron diffraction and high-resolution electron microscopy. The crystal structure of κ-Al_2O_3 has been found to be orthorhombic, space group $Pna2_1$. The lattice parameters are $a = 4{\cdot}69$, $b = 8{\cdot}18$ and $c = 8{\cdot}87$ Å. The volume is $340{\cdot}3$ Å^3 and the density is $\sim 3{\cdot}98$ g cm^{-3}, $Z = 8$. Three different variants of κ-Al_2O_3 domains give rise to a false superlattice which can be described by a hexagonal structure. An atomic model for κ-Al_2O_3 based on the experimental results has been constructed.

Introduction

Alumina or aluminium oxide (Al_2O_3) is an important material used in many different applications. A typical example is CVD (chemical vapour deposition) coatings of alumina on cemented carbides. CVD Al_2O_3 coatings combined with TiC provide cemented carbide tools with increased wear resistance for metal cutting applications. Often the coatings will increase the effective operating life time by 3–8 times compared to tools without coatings. Alumina is a well known compound with seven different crystal modifications of pure Al_2O_3, *i.e.* α, κ, δ, γ, θ, η and χ. Only one of them, α-Al_2O_3, has an established crystal structure. In addition to the stable α-Al_2O_3, only the κ-Al_2O_3 modification is of any great interest for CVD applications. Although the existence of κ-Al_2O_3 has been known for almost 40 years, its crystal structure had not been determined with certainty.

The dehydration of tohdite, $5Al_2O_3.H_2O$, gave the transformation series (Okumiya, Yamaguchi, Yamada & Ono, 1971):

$$5Al_2O_3.H_2O \rightarrow \kappa'\text{-}Al_2O_3 \rightarrow \kappa\text{-}Al_2O_3 \rightarrow \alpha\text{-}Al_2O_3.$$

By thermal analyses (DTA and TGA) a single endothermic reaction in the temperature range 975–1075 K and one exothermic reaction at 1275 K were found. The exothermic reaction at 1275 K was revealed by X-ray diffraction to be the formation of α-Al_2O_3. The endothermic reaction at 975–1075 K would correspond to the formation of κ'-Al_2O_3 and κ-Al_2O_3. The tohdite has a hexagonal crystal structure and closed-packed oxygen ion layers with an *ABAC*... stacking sequence (Krischner, 1966). The aluminium ions occupy both octahedral and tetrahedral positions. The κ'-Al_2O_3 structure was revealed by X-ray diffraction to be similar to tohdite, *i.e.* *ABAC*... close packing of oxygen ion layers and randomly distributed aluminium ions over both the octahedral and tetrahedral positions (Okumiya, Yamaguchi, Yamada & Ono, 1971). So κ'-Al_2O_3 was described as a partly cationic redistributed structure of tohdite and as an unstable intermediate phase in the transformation from tohdite to κ-Al_2O_3. Moreover, X-ray diffraction data from κ-Al_2O_3 were very similar to data from κ'-Al_2O_3 (Okumiya, Yamaguchi, Yamada & Ono, 1971). The additional reflections that appeared from κ-Al_2O_3 were explained by the distribution of Al^{3+} ions.

Previous investigators proposed a hexagonal or triclinic crystal system for κ-Al_2O_3 (Landolt–Börnstein, 1975) based on X-ray diffraction studies. Saalfeld (1960) proposed a cell size of $a = 9{\cdot}71$ and $c = 17{\cdot}86$ Å for a hexagonal unit cell, while Okumiya, Yamaguchi, Yamada & Ono (1971) interpreted their electron diffraction and X-ray diffraction data as arising from a similar unit cell to that proposed by Saalfeld but with a much shorter c axis: $a = 9{\cdot}599$ and $c = 9{\cdot}024$ Å. Another worker suggested the hexagonal unit cell to be $a = 9{\cdot}71$ or $a = 16{\cdot}78$ Å but the c axis was not determined (Brindley & Choe, 1961). However, there is no consensus as to κ-Al_2O_3 unit-cell parameters. Moreover, no crystal symmetry of κ-Al_2O_3 (*i.e.* point group and space group) was determined nor were the atomic coordinates in κ-Al_2O_3 even suggested.

One of the reasons why the crystal structure and the lattice parameters of κ-Al_2O_3 are still uncertain is the difficulty in obtaining single-phase samples which are sufficiently large and free from defects in order to obtain enough diffraction intensity data by X-ray (ASTM file No. 4-0878) or conventional electron

* Present address: Research and Development Centre, AB Sandvik Steel, S-811 81 Sandviken, Sweden.

0108-7681/91/040425-09$03.00

diffraction. In order to perform X-ray diffraction experiments, specimens with a size of about 0·1 mm^3 are required and even for conventional electron diffraction experiments, the size of the specimen must be a few micrometers. However, the convergent-beam electron diffraction (CBED) technique makes it possible to obtain crystallographic information from a very localized area which can be as small as a few hundred ångstroms (Williams, 1987). CBED can supply three-dimensional information from a very small area as a result of the angular variation of intensity within the disc of a given order of Bragg reflection (Steeds, 1979). This three-dimensional information enables determination of crystal symmetry point groups and space groups. By investigating the symmetries of CBED patterns, which can be described by 31 diffraction groups, the point groups can be determined (Buxton, Eades, Steeds & Rackham, 1967). Screw axes and glide planes often give rise to dark lines in CBED, which are kinematically forbidden. These lines of absent intensity are called 'dynamic absences' or 'Gjønnes–Moodie lines' (G–M lines) (Gjønnes & Moodie, 1965). The G–M lines can be used very effectively for space-group determination (Tanaka & Sekii, 1982).

Experimental

The material used in the present study was AB Sandvik Coromant's TiC–Al_2O_3–TiN coated cutting tool inserts of type GC 415 and GC 3015.

Thin foils for transmission electron microscopy studies were prepared from both the specimens, which were taken from the plane of the coating (plane view specimen) and the perpendicular direction to the coating (cross section specimen), by ion-beam thinning. The techniques concerning the preparation of the thin foils are described elsewhere (Skogsmo, 1989).

Ion-beam milling was carried out in a Gatan dual ion-milling system using argon ions with an energy of 4 kV. The thin foils were examined in a Jeol 2000FX TEM/STEM microscope, operating at 200 kV, and occasionally a few kV lower accelerating voltage was used in order to check if dynamic absences appeared. The CBED patterns, which are presented in this work, were taken at 200 kV.

A double-tilt Gatan cooling holder was used with the specimens cooled to about liquid nitrogen temperature in order to reduce the effect of thermal vibration and to minimize hydrocarbon contamination.

In order to determine the unit cell and structure of the κ-Al_2O_3 crystal lattice, a procedure involving the geometric projection of the electron diffraction patterns (Kuo, Ye & Wu, 1983) was used. Reflections from TiN were used as internal standards for the calibration of the camera constant.

Results

In Fig. 1 a bright-field image shows a cross-section specimen, which is perpendicular to the CVD growth direction. The different layers can be seen in this specimen, *i.e.* WC—Co, TiC and κ-Al_2O_3 layers. Moreover, κ-Al_2O_3 grains show an elongated morphology in this direction. Plane-view specimens, which were cut in the parallel direction to the cross-section specimen and therefore are parallel to the CVD growth direction, show that κ-Al_2O_3 grains are equiaxed in this direction. Thus, the images of κ-Al_2O_3 in the two perpendicular directions revealed that κ-Al_2O_3 has a columnar grain structure. The axes of the columnar grains are parallel to the CVD direction and the grains have diameters of about 1 μm and lengths are about the same as the thickness of the κ-Al_2O_3 coating which is several micrometers.

A selected-area electron diffraction (SAED) pattern obtained from a κ-Al_2O_3 grain of the plane-view specimen is shown in Fig. 2. This pattern shows a pseudo-sixfold rotation symmetry. This pattern had previously been indexed as a [0001] zone axis pattern from an hexagonal structure (Brindley & Choe, 1961). A high-resolution lattice image is shown in Fig. 3, with an inserted SAED pattern, which indicates the beams used for forming this image. It can be seen that the image consists of three sets of lattices, with a lattice spacing of 8·18 Å, which are related to each other by 120° rotations. This is direct evidence that the pseudo-sixfold rotation symmetry pattern was not formed from one single grain but from three grains which were related to each other

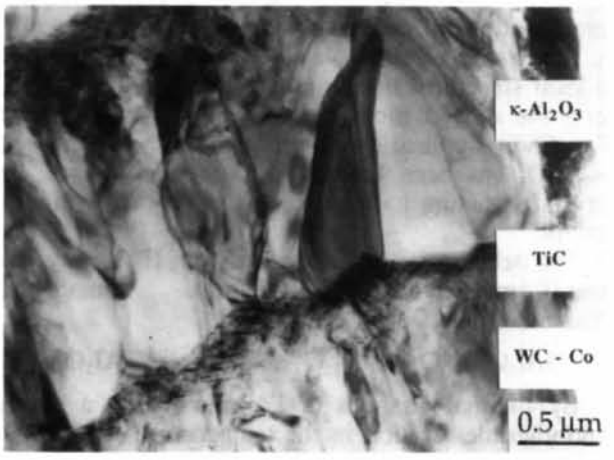

Fig. 1. Bright-field image of a cross-sectional specimen showing that κ-Al_2O_3 grains are elongated in the CVD growth direction.

by rotation of 120° around the axis, which is parallel to the electron beam. Furthermore, when placing a small electron beam (electron beam diameters ~100 Å) on one of the grains marked as *A*, *B* and *C* in Fig. 3, a small-angle CBED pattern was obtained as shown in Fig. 4(*a*). This type of pattern cannot be indexed by the proposed hexagonal structure model suggested by previous investigators. The SAED pattern shown in Fig. 2 is in fact a superimposed pattern of the three separate patterns shown in Fig. 4(*a*). By tilting the crystal around the two shortest reciprocal lattice vectors in the pattern shown in Fig. 4(*a*), a series of SAED patterns were then obtained. By projection of the patterns onto the planes, which are perpendicular to the tilting axes, a reciprocal unit cell was obtained. In real space, a primitive Bravais lattice and an orthorhombic crystal structure was then deduced. The lattice parameters obtained are $a = 4{\cdot}69$, $b = 8{\cdot}18$ and $c = 8{\cdot}87$ Å. The volume is calculated to be $340{\cdot}3$ Å^3.

Fig. 2. SAED pattern taken from the plane-view specimen showing a pseudo-sixfold rotation symmetry.

The CBED pattern shown in Fig. 4(*a*) is indexed as the [001] zone axis. Furthermore, from the pattern shown in Fig. 4(*a*) the diffraction condition was revealed as follows: *h*00: $h = 2n$ and 0*k*0: $k = 2n$ ($n = \pm 1, \pm 2, \ldots$).

It can also be seen from the higher-order Laue zone (HOLZ) in the [001] pattern (Fig. 4*b*) that the reflections in the HOLZ have no displacement from the zero-order Laue zone (ZOLZ) and their positions are just a simple repeat of the ZOLZ. This confirmed that κ-Al_2O_3 has a primitive Bravais lattice (Williams, 1987). Furthermore, from the measurement of the radius of the HOLZ ring, the distance between the ZOLZ and the HOLZ can be calculated (Steeds & Vincent, 1983): $H_{001} = 1/r_{001} = 1/8{\cdot}87$ Å^{-1}, in which $r_{001} = c$. Hence, together with the measurements of the lattice parameters *a* and *b* from the [001] pattern the results confirm the determination of the unit cell.

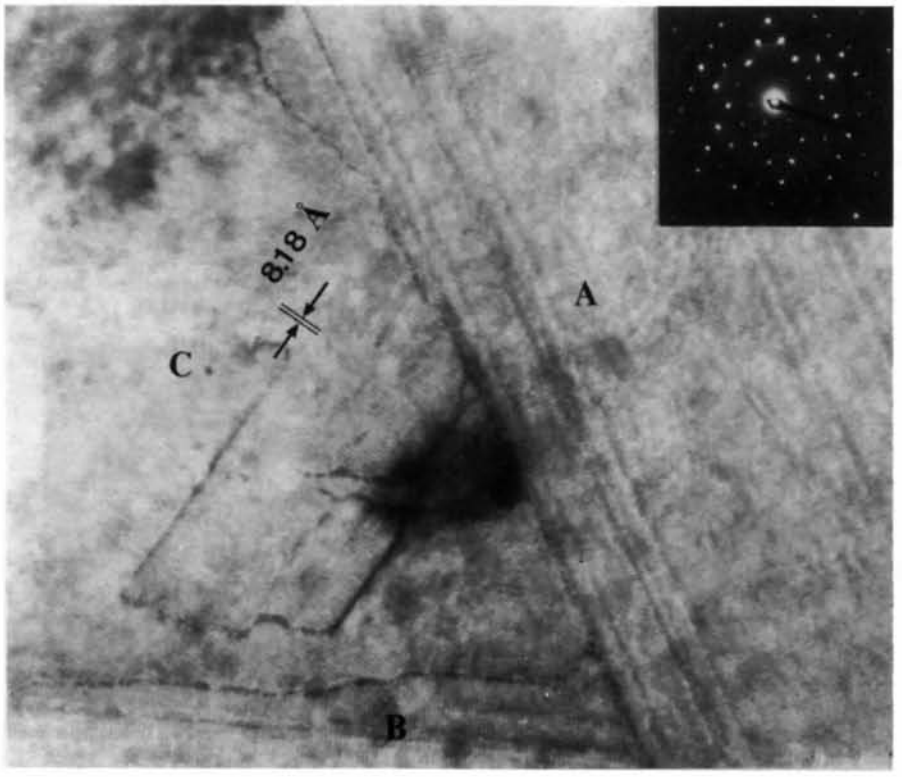

Fig. 3. High-resolution lattice image formed by the inserted SAED pattern was obtained from the plane-view specimen. It shows three domains related by 120° rotations.

The symmetries of the bright-field disc and the dark-field discs (Buxton, Eades, Steeds & Rackham, 1967) can hardly be recognized from the [001] CBED pattern shown in Fig. 4, because the unit cell of the κ-Al_2O_3 crystal is very large and the discs in CBED are either overlapped or so small. However, the whole-pattern symmetry (or the symmetry of the complete zone-axis pattern) can be used to deduce the crystallographic point group of κ-Al_2O_3. The WP symmetry can be seen from Fig. 4(*c*) (taken with a larger electron beam) as 2*mm*, indicating the presence of both (100) and (010) mirrors, which leaves the possible crystal point groups of κ-Al_2O_3 as *mmm* and *mm*2 (Buxton, Eades, Steeds & Rackham, 1967).

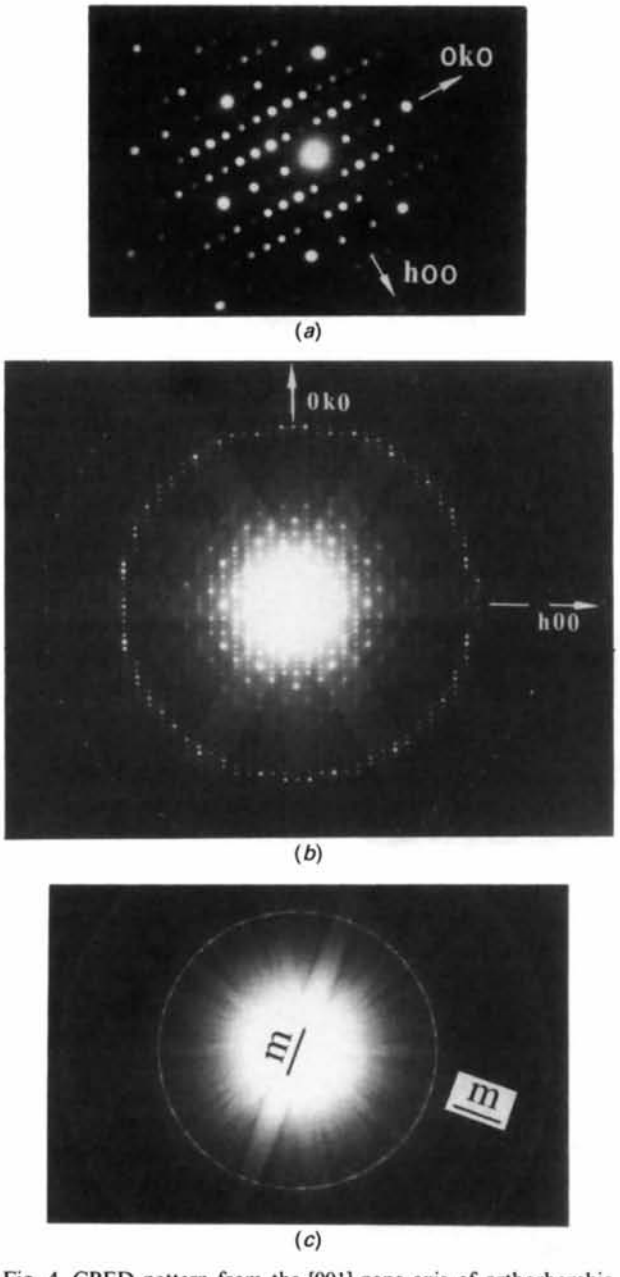

(*a*) (*b*) (*c*)

Fig. 4. CBED pattern from the [001] zone axis of orthorhombic κ-Al_2O_3. (*a*) The zero-order Laue zone (a small electron beam with a diameter ~100 Å); (*b*) the whole pattern (a small electron beam with a diameter ~100 Å); (*c*) the whole pattern (a larger electron beam) showing whole-pattern symmetry of 2*mm*.

Two SAED patterns taken from the cross-section specimens are shown in Figs. 5 and 6. They were indexed as [100] and [010] zone axes respectively, if the diffraction conditions are considered as $0k0$: $k = 2n$, $00l$: $l = 2n$ and $0kl$: $k + l = 2n$ ($n = \pm 1, \pm 2, \ldots$).

The CBED pattern from the [110] zone axis (Fig. 7) shows no higher symmetry than 1, which indicates the absence of the (001) mirror. Therefore, it can be concluded from the WP symmetries of different zone axes that κ-Al_2O_3 has the point-group symmetry of *mm*2 (Buxton, Eades, Steeds & Rackham, 1967).

There are ten space groups which have the point group of *mm*2 and are of the primitive Bravais lattice type; these are (Hahn, 1983; Tanaka & Terauchi, 1985):

*Pmm*2 (No. 25)	*Pcc*2 (No. 27)	*Pmc*2_1 (No. 26)
*Pma*2 (No. 28)	*Pnc*2 (No. 30)	*Pca*2_1 (No. 29)
*Pba*2 (No. 32)	*Pnn*2 (No. 34)	*Pmn*2_1 (No. 31)
		Pna2_1 (No. 33).

Fig. 5. SAED pattern taken from the cross-sectional specimen showing the [100] zone axis of κ-Al_2O_3.

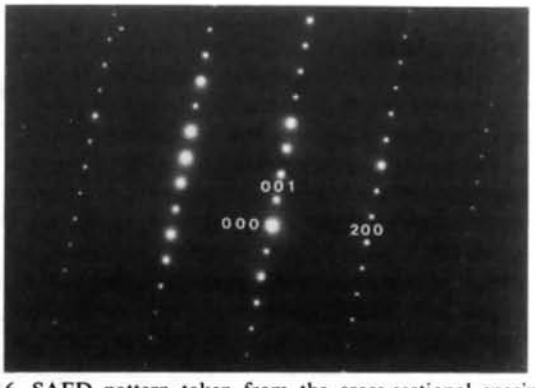

Fig. 6. SAED pattern taken from the cross-sectional specimen showing the [100] zone axis of κ-Al_2O_3.

However, from the CBED pattern shown in Fig. 8 G–M lines (or dynamical absences) can be seen in the (00l) discs where l is an odd number. The occurrence of these dynamical absences in kinematically forbidden reflections can be used to confirm the presence of screw axes and glide planes in the structure. In the present case, it is the existence of a 2_1 screw axis along the c axis (Steeds & Vincent, 1983; Tanaka & Terauchi, 1985; Tanaka, Terauchi & Kaneyama, 1988). This means that the possible space groups are those which have a 2_1 screw axis, *i.e.* $Pmc2_1$ (No. 26), $Pca2_1$ (No. 29), $Pmn2_1$ (No. 31) and $Pna2_1$ (No. 33). Considering the diffraction conditions revealed by the patterns shown in Figs. 4(*a*), 5 and 6, *i.e.* $h00$: $h = 2n$, $0k0$: $k = 2n$, $00l$: $l = 2n$ and $0kl$: $k + l = 2n$ ($n = \pm 1, \pm 2, \ldots$), only two out of the ten space groups are possible. They are $Pna2_1$ (No. 33) and $Pnn2$ (No. 34) (Hahn, 1983). As CBED revealed the presence of the screw axis 2_1 along the c axis, this leaves the only possible crystallographic space group of κ-Al_2O_3 to be $Pna2_1$ (No. 33).

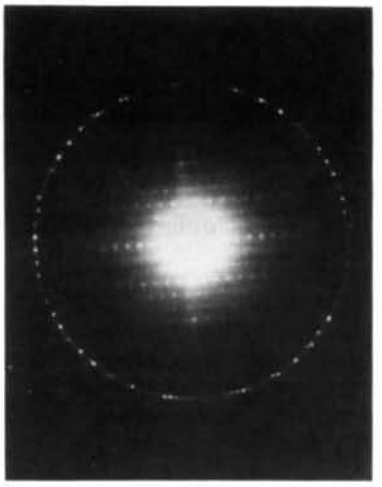

Fig. 7. CBED pattern from the [110] zone axis of κ-Al_2O_3 showing the whole-pattern symmetry of only 1.

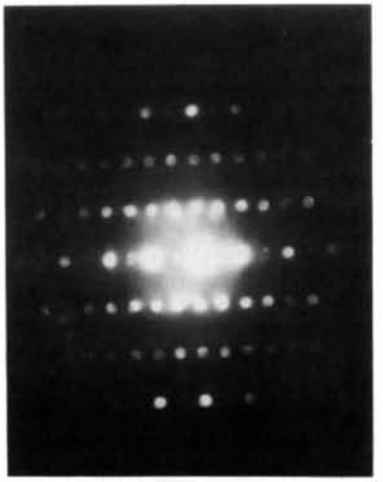

Fig. 8. The zero-order Laue zone of the CBED pattern in Fig. 7 showing G–M lines in the discs of (00l), where l is an odd number.

From the CBED pattern taken from the [010] zone axis shown in Fig. 9, it can be seen in the ZOLZ that there are G–M lines in the discs of (00l) where l is an odd number. This indicates the existence of 2_1 along the c axis. In the HOLZ ring there is a G–M line in the (0,1,26) disc, which indicates the presence of the n glide plane perpendicular to the a axis (Tanaka, Terauchi & Kaneyama, 1988). In addition, the a glide on the (010) plane is visible by comparison of the spacing of ZOLZ and FOLZ reflections along the [100] direction where the reflections of ($h0l$) are missing in ZOLZ when h is an odd number (Hahn, 1983). These results confirm the space group of κ-Al_2O_3 to be $Pna2_1$ (No. 33).

Atomic model

By comparing the lattice parameters of κ-Al_2O_3 with those of α-Al_2O_3 (Pauling & Hendricks, 1925; Newnham & de Haan, 1962; Kronberg, 1957), it can be seen that there is a simple transformation between the two structures, *i.e.*

$a_\kappa \simeq r_{[100]\alpha} = a_\alpha$	$a_\kappa = 4{\cdot}69$ Å	$a_\alpha = 4{\cdot}759$ Å
$b_\kappa \simeq r_{[120]\alpha} = 3^{1/2} a_\alpha$	$b_\kappa = 8{\cdot}18$ Å	$3^{1/2} a_\alpha = 8{\cdot}243$ Å
$c_\kappa \simeq \frac{2}{3} r_{[001]\alpha} = \frac{2}{3} c_\alpha$	$c_\kappa = 8{\cdot}87$ Å	$\frac{2}{3} c_\alpha = 8{\cdot}661$ Å

where the subscripts κ and α are referred to κ-Al_2O_3 and α-Al_2O_3 respectively, and $r_{[uvw]\alpha}$ is a lattice vector of α-Al_2O_3. For α-Al_2O_3 the Bravais index is used for convenience, *i.e.* [100], [120] and [001], and these are $[2\bar{1}\bar{1}0]$, $[01\bar{1}0]$ and [0001] respectively in the Miller–Bravais index system.

Considering the accuracy of determination of the lattice parameters by electron diffraction, it can be seen that κ-Al_2O_3 has the same dimensions as α-Al_2O_3 in the plane perpendicular to the c axis, while it is expanded in the c-axis direction compared to α-Al_2O_3. This implies that in κ-Al_2O_3 the framework is the same as for α-Al_2O_3, *i.e.* close-packed O^{2-} ions. The stacking of the close-packed O^{2-} ions in α-Al_2O_3 is *ABAB*... which gives the space group $P6_3mmc$ (No. 194) (Pauling & Hendricks, 1925). Then Al^{3+} ions occupying two-thirds of the octahedral positions have three different positions, *i.e.* α, β, γ. Thus the crystal of α-Al_2O_3 has a stacking sequence of $A\alpha B\beta A\gamma B\alpha A\beta B\gamma A\alpha \ldots$ which gives α-Al_2O_3 the space group $R\bar{3}c$ (No. 167). Fig. 10(*a*) shows the stacking in the projection along the $[1\bar{2}10]$ direction of α-Al_2O_3.

If O^{2-} ions in κ-Al_2O_3 are close packed and the equation $c_\kappa = \frac{2}{3} c_\alpha$ is considered then the possible

stacking sequence of the close-packed O^{2-} ion layers can be either *ABAB* or *ABAC* and both can have the same space group $P6_3mmc$. When the Al^{3+} ions are placed into the interstitial positions there are two alternatives, *i.e.* $A\alpha B\alpha A\beta B\beta A\alpha$ and $A\alpha B\alpha A\beta' C\beta' A\alpha$, which can keep the length of the *c* axis and the reasonable stacking of the Al^{3+} ion layers (β and β' represent the octahedral and tetrahedral positions respectively). However, because in the former stacking the twofold rotation symmetry operation along the *c* axis is not preserved as in the later case for the stacking of κ-Al_2O_3, the stacking sequence for κ-Al_2O_3 must therefore be $A\alpha B\alpha A\beta' C\beta' A\alpha$. This stacking sequence is shown in Fig. 10(*b*). It can be seen that Al^{3+} ions occupy both octahedral (α) and tetrahedral (β') interstitial positions. This arrangement has broken down the 6_3 screw axis of the O^{2-} substructure but has maintained the symmetry of $Pna2_1$ (No. 33) as one of the subgroups of space group $P6_3mmc$. Thus, this arrangement of ions has the symmetry elements of the κ-Al_2O_3 structure.

It is known that there are three variants of transformation from hexagonal coordinates to orthogonal ones (Hahn, 1983), *i.e.* three choices of orthogonal axes. In the case of the κ-Al_2O_3 structure there are three different arrangements for Al^{3+} ions in the O^{2-} ions framework of *ABAC*... stacking and each one gives exactly the same crystal structure as the others but a different orientation from one to the others. These three different arrangements are

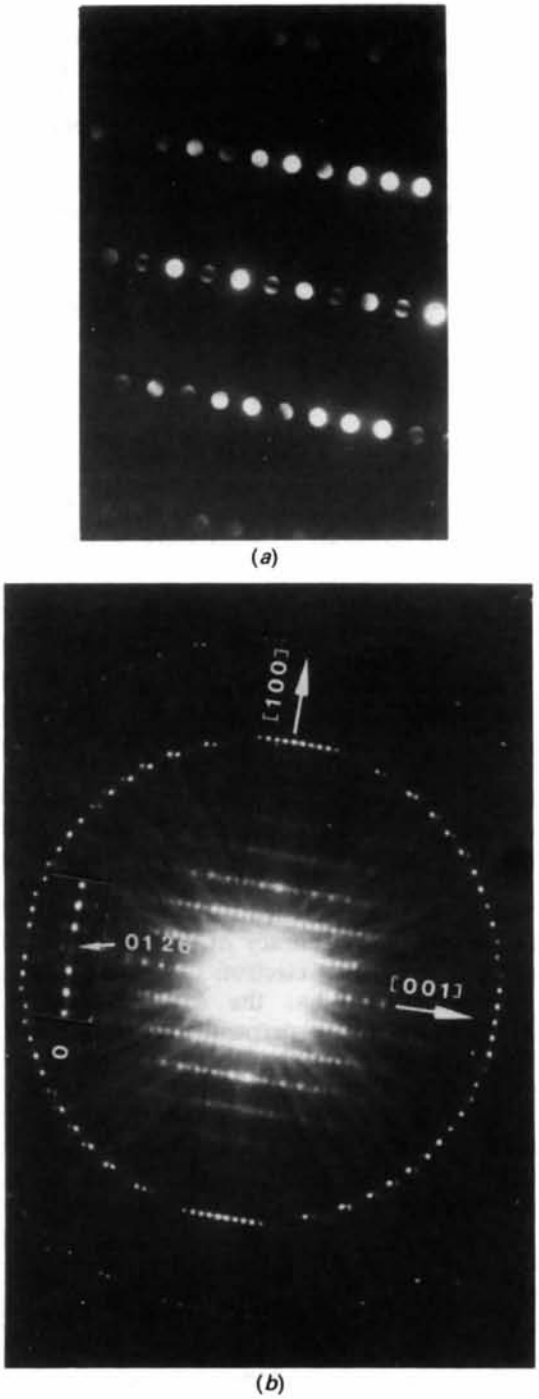

Fig. 9. CBED pattern of κ-Al_2O_3 from the [010] zone axis showing G–M lines both in (*a*) the zero-order Laue zone and (*b*) the higher-order Laue zone.

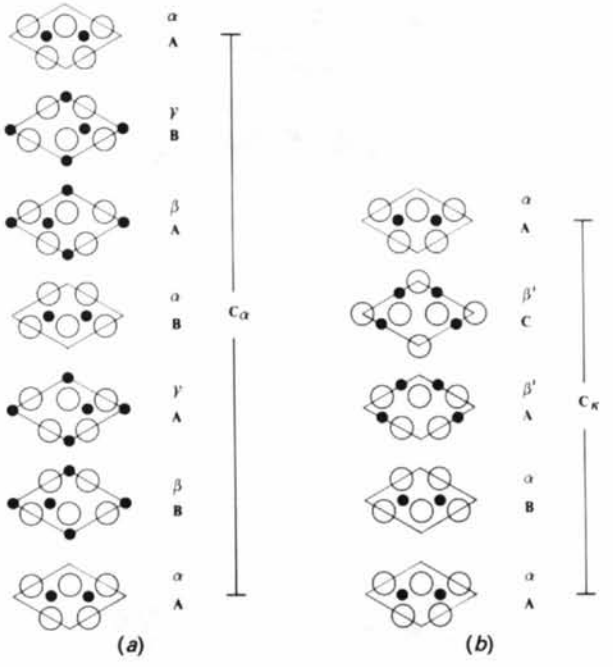

Fig. 10. The stacking sequence along *c* axes in α-Al_2O_3 and κ-Al_2O_3. Empty circles represent O^{2-} ions and filled circles Al^{3+} ions. *A*, *B* and *C* are O^{2-} layers, α, β and γ are the Al^{3+} layers occupying octahedral interstitial positions and β' the Al^{3+} layers occupying tetrahedral ones. (*a*) On the projection along the $[1\bar{2}10]$ direction of α-Al_2O_3; (*b*) on the projection along the [100] direction of κ-Al_2O_3.

related by rotation of 120° to each other, and each arrangement can be defined as a domain. Furthermore, if three such domains grow together a false superlattice will result. This false superlattice can be described by a hexagonal unit cell with lattice parameters $a = 9{\cdot}44$ and $c = 8{\cdot}87$ Å. This is exactly the structure which can be deduced from the SAED pattern in Fig. 3. This pattern can be indexed as the [0001] zone axis of the hexagonal lattice.

Each of the domains in κ-Al_2O_3 can be related to the other domains by a twinning operation through their {110} planes. The domain boundaries would then be twin boundaries. This structure is illustrated in the high-resolution lattice image shown in Fig. 3. If the twins form in small size and with a more or less regular spacing a long periodicity along the a axis or the b axis can be introduced. Fig. 11(a) shows the lattice image of κ-Al_2O_3. It can be seen that there are regular spacings, for example, as indicated by A and B, and irregular ones marked as C, D and E. The long periodicities resulting from the regular spacings have been shown to give extra spots between (100) reflections [see Fig. 11(b)]. The irregular spacings such as C, D and E give rise to streaking as shown in Fig. 11(b).

In order to simulate the X-ray diffraction and electron diffraction data, the atomic coordinates have to be determined. This may be done by using the transformation as described by the matrix (Hahn, 1983):

$$(a\ b\ c)_\alpha \begin{pmatrix} 1 & 1 & 0 \\ 0 & 2 & 0 \\ 0 & 0 & \frac{2}{3} \end{pmatrix} = (a\ b\ c)_\kappa$$

and

$$(a\ b\ c)_\alpha = (a\ b\ c)_\kappa \begin{pmatrix} 1 & -\frac{1}{2} & 0 \\ 0 & \frac{1}{2} & 0 \\ 0 & 0 & \frac{3}{2} \end{pmatrix}$$

plus the shift of the origin. Then through

$$(x\ y\ z)_\alpha \mathbf{P}^{-1} = (x\ y\ z)_\kappa,$$

$$\mathbf{P} = \begin{pmatrix} 1 & 1 & 0 \\ 0 & 2 & 0 \\ 0 & 0 & \frac{2}{3} \end{pmatrix}$$

and

$$\mathbf{P}^{-1} = \begin{pmatrix} 1 & -\frac{1}{2} & 0 \\ 0 & \frac{1}{2} & 0 \\ 0 & 0 & \frac{3}{2} \end{pmatrix}$$

the atomic coordinates of κ-Al_2O_3 may be calculated. Since the ratio of the unit-cell volumes of the κ-Al_2O_3 to the α-Al_2O_3 is 4/3, there are 24 O^{2-} and 16 Al^{3+} in the κ-Al_2O_3. Hence, there are six nonequivalent positions for O^{2-} and four nonequivalent positions for Al^{3+}. By operating the symmetric operations in space group $Pna2_1$, the atomic coordinates can be obtained for this model. From the model the density of κ-Al_2O_3 can be calculated as 3·98 g cm^{-3}.

Diffraction experiments and intensity simulation are in progress in order to prove the atomic model.

Discussion

Though the description of the space-group determination of the κ-Al_2O_3 crystal structure began with

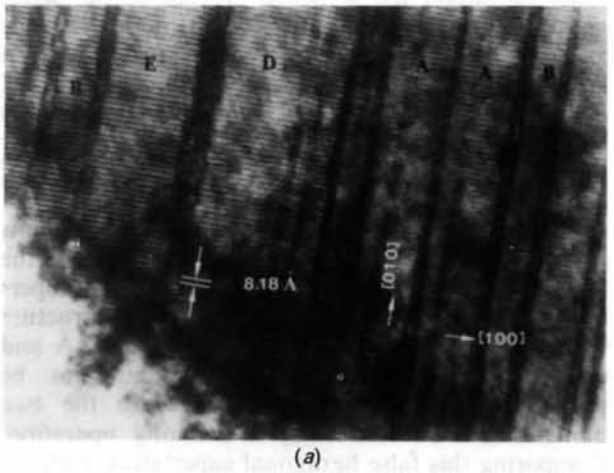

(a)

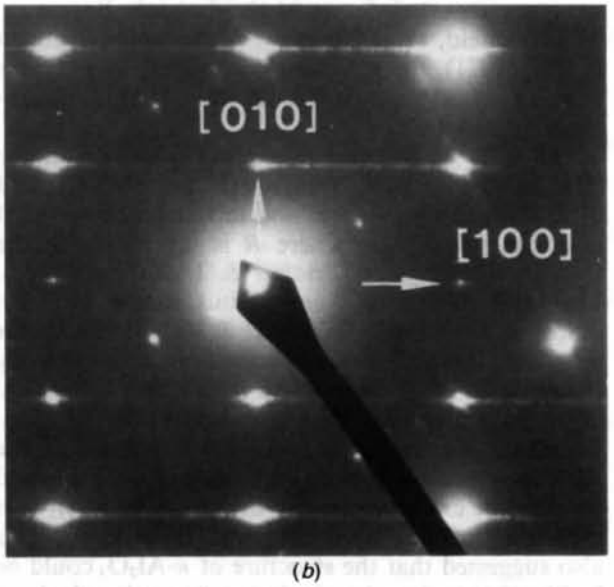

(b)

Fig. 11. (a) Lattice image of κ-Al_2O_3 showing the regular (marked as A and B) and irregular spacings (marked as C, D and E) between the twins. (b) Extra reflections and streakings along the (100) direction of the SAED pattern from κ-Al_2O_3.

determination of the unit-cell geometry, in practice, the determination of the space group of the κ-Al_2O_3 crystal started by searching the symmetry of SAED patterns from different orientations or projection diffraction symmetries (Buxton, Eades, Steeds & Rackham, 1967). As the cell geometry is dependent upon the crystal system to which the crystal structure belongs and the crystal system is defined by its Laue class, *i.e.* the lattice symmetry (Hahn, 1983), the Laue class can readily be determined from projection diffraction symmetries of electron diffraction patterns from different orientations.

For orthorhombic space groups, the symbols of space groups have six settings of the same unit cell, which correspond to six different settings of lattice bases. In this case, the priority rule was applied, in order to obtain the standard symbol of the space group (Hahn, 1983). That is, when more than one kind of symmetry element is present for a given symmetry direction, the choice is made in order of descending priority *m*, *a*, *b*, *c*, *n*, *d*, and rotation axes before screw axes. This is why the space group for the κ-Al_2O_3 crystal structure is $Pna2_1$ instead of either $Pbn2_1$, $P2_1nb$, $P2_1cn$ or $Pc2_1n$.

The three different variants of κ-Al_2O_3 domains give rise to a false superlattice, which can have the SAED pattern shown in Fig. 2. This false superlattice can be described by a hexagonal structure with lattice parameters $a = 9{\cdot}44$ and $c = 8{\cdot}87$ Å and each boundary between two domains can be described as a twin boundary because the two domains can be related by a twinning operation. Comparing this false hexagonal superlattice with the structure reported for κ-Al_2O_3 (Landolt–Börnstein, 1975; Saalfeld, 1960; Okumiya, Yamaguchi, Yamada & Ono, 1971), the structure determined by previous workers is a superlattice of the κ-Al_2O_3 orthorhombic structure.

The sizes of the two interstitial positions in the close-packed oxygen framework are $0{\cdot}414R$ and $0{\cdot}225R$ for the octahedral and tetrahedral interstitial positions respectively where R is the radius of the O^{2-} ion (Vainshtein, Fridkin & Indenbom, 1982). The ratio of the Al^{3+} ion radius to the O^{2-} ion radius is $0{\cdot}53/1{\cdot}40 = 0{\cdot}38$ and $0{\cdot}39/1{\cdot}38 = 0{\cdot}28$ for the six and four coordinations respectively (Richerson, 1982). Hence the tetrahedral interstitial positions are smaller than the size of the Al^{3+} ion. Therefore, an expansion would be expected if the Al^{3+} ions occupy this type of position. This could provide the explanation why the lattice of κ-Al_2O_3 is expanded in the *c* axis compared to α-Al_2O_3. This also suggested that the structure of κ-Al_2O_3 could be highly distorted and a deviation from the idealized positions proposed would be expected.

κ-Al_2O_3 was reported to have a higher thermal stability than κ'-Al_2O_3 and this was attributed to stabilization by impurities (Krischner, 1966). However, investigations by analytical electron microscopy, atom-probe (Skogsmo, Henjered & Nordén 1984; Skogsmo & Nordén, 1985; Vuorinen & Skogsmo, 1988) and scanning Auger microprobe analysis (Skogsmo, Liu, Chatfield & Nordén, 1989) showed no significant amounts of impurities in either α-Al_2O_3 or κ-Al_2O_3 formed by CVD. This implies that the structure of κ-Al_2O_3 must be relatively stable even without detectable amounts of impurities. Thus, the alternation of the octahedral and tetrahedral positions for aluminium ions in the close-packed *ABAC*... oxygen layers would be energetically favourable. It is that the ordered Al^{3+} ions in κ-Al_2O_3 are more stable than the disordered ones in κ'-Al_2O_3.

The α-Al_2O_3 grains were found to be equiaxed and randomly oriented (Skogsmo, Liu, Chatfield & Nordén, 1989) while the κ-Al_2O_3 grains showed a columnar morphology and were preferentially oriented. This indicates that κ-Al_2O_3 grows by depositing each oxygen ion layer and aluminium ion layer alternately while α-Al_2O_3 does not grow in the same way. The transformation of κ-Al_2O_3 to α-Al_2O_3 will involve the rearrangement of oxygen and aluminium ions.

We thank Professor D. B. Williams for reading the manuscript and Dr H. Nordén and Professor G. L. Dunlop at Chalmers and Dr C. Chatfield at AB Sandvik Coromant for encouragement during the work. We also thank the referees for their critical comments. The work was financially supported by the Swedish National Board for Technical Development (STU).

References

BRINDLEY, G. W. & CHOE, J. O. (1961). *Am. Mineral.* **46**, 771–785.
BUXTON, B. F., EADES, J. A., STEEDS, J. W. & RACKHAM, G. M. (1967). *Philos. Trans. R. Soc. London Ser. A*, **281**, 171–194.
GJØNNES, J. & MOODIE, A. F. (1965). *Acta Cryst.* **19**, 65–67.
HAHN, T. (1983). Editor. *International Tables for Crystallography*, Vol. A, pp. 27–30, 40–48, 53, 70–79, 590–591. Dordrecht: Kluwer Academic Publishers.
KRISCHNER, H. (1966). *Ber. Dtsch. Keram. Ges.* **43**, 479–484.
KRONBERG, M. L. (1957). *Acta Metall.* **5**, 507–524.
KUO, K. H., YE, H. Q. & WU, Y. K. (1983). *Electron Diffraction Pattern with its Applications of Crystallography*, p. 241. Beijing: Science Press. (In Chinese.)
LANDOLT–BÖRNSTEIN (1975). *Crystal and Solid State Physics*, Vol. 7, p. 61. Berlin: Springer Verlag.
NEWNHAM, R. E. & DE HAAN, Y. M. (1962). *Z. Kristallogr.* **117**, 235–237.
OKUMIYA, M., YAMAGUCHI, G., YAMADA, O. & ONO, S. (1971). *Bull. Chem. Soc. Jpn*, **44**, 418–423.
PAULING, L. & HENDRICKS, S. B. (1925). *J. Am. Chem. Soc.* **47**, 781–790.
RICHERSON, D. W. (1982). *Modern Ceramic Engineering*, p. 9. New York: Marcel Dekker.

SAALFELD, H. (1960). *Neues. Jahrb. Mineral. Abh.* **95**, 1–87.
SKOGSMO, J. (1989). PhD Thesis, Chalmers Univ. of Technology, Sweden.
SKOGSMO, J., HENJERED, A. & NORDÉN, H. (1984). *J. Phys. (Paris) Colloq.* **9**(45), 447–451.
SKOGSMO, J., LIU, P., CHATFIELD, C. & NORDÉN, H. (1989). *Proceedings of the Twelfth International Plansee Seminar* 1989, Vol. 3, edited by H. BILDSTEIN & H. M. ORTNER, pp. 129–142. Reutte, Tirol, Austria: Metallwerk Plansee GMBH.
SKOGSMO, J. & NORDÉN, H. (1985). *Proceedings of the Fifth European Conference on CVD*, edited by J.-O. CARLSSON & J. LINDSTRÖM, pp. 364–370. Uppsala Univ., Sweden.
STEEDS, J. W. (1979). *Introduction to Analytical Electron Microscopy*, edited by J. J. HREN, J. I. GOLDSTEIN & D. C. JOY, ch. 15, pp. 387–422. New York: Plenum Press.
STEEDS, J. W. & VINCENT, R. (1983). *J. Appl. Cryst.* **16**, 317–324.
TANAKA, M. & SEKII, H. (1982). *Electron Microscopy* 1982, *Proceedings of the Tenth International Congress on Electron Microscopy*, Vol. 1, pp. 631–632. Hamburg: Offizin Paul Hartung.
TANAKA, M. & TERAUCHI, M. (1985). *Convergent-Beam Electron Diffraction*, pp. 160–173. Tokyo: Jeol Ltd.
TANAKA, M., TERAUCHI, M. & KANEYAMA, T. (1988). *Convergent-Beam Electron Diffraction*, Vol. 2, pp. 214–225. Tokyo: Jeol Ltd.
VAINSHTEIN, B. K., FRIDKIN, V. M. & INDENBOM, V. L. (1982). Editors. *Modern Crystallography*, Vol. 2, *Structure of Crystals*, pp. 70–114, Berlin: Springer Verlag.
VUORINEN, S. & SKOGSMO, J. (1988). *Proceedings of the First International Conference on Surface Modification Techniques*, pp. 143–168. Phoenix, Arizona.
WILLIAMS, D. B. (1987). *Practical Analytical Electron Microscopy in Materials Science*, revised ed., pp. 1, 127–133. Princeton, New Jersey: Electron Optics Publishing Group.

Acta Cryst. (1991). B47, 433–439

Inorganic Structure Types with Revised Space Groups. I*

BY KARIN CENZUAL, LOUISE M. GELATO, MARINELLA PENZO AND ERWIN PARTHÉ

Laboratoire de Cristallographie aux Rayons X, Université de Genève, 24 quai E. Ansermet, CH-1211 Geneva 4, Switzerland

(*Received* 5 *September* 1990; *accepted* 15 *January* 1991)

Abstract

Standardized data sets in space groups which consider all symmetry elements in the structure are given for the following structure types, originally reported in space groups with lower symmetry or with larger unit cells (numbers of original and new space group are indicated within parentheses): Ag_3TlTe_2 (53→65), Au_3Cd (107→139), Ca_3Hg (217→221, $\frac{1}{4}$ volume of primitive cell), $CeZn_3$ (62→63), $CoGe_2$ (41→64), CuAu phase I (123→123, $\frac{1}{2}$ cell volume), $Cu_{10}Sb_3$ (147→176), GaSe 2*H* ε (174→187), InSe II (10→12), LaB_2C_2 (112→131), α-Li_3BN_2 (94→136), $Li_{6.45}Mn_3As_4$ (16→49 or 67), Li_7Pb_2 (150→164), $LiPd_2$ (10→10, $\frac{1}{2}$ cell volume), LiRh (174→187), $MgAu_{3-x}$ (38→63), Mg_3In (146→166), Mn_2AlB_2 (21→65), Mn_3As (59→63), MnBi QHT (17→51), $Mn(Bi_{0.85}Sb_{0.15})$ (17→51), Na_2HgO_2 (97→139), $Na_{1-x}TiS_2$ (146→160), $NbD_{0.95}$ (48→66), θ-Ni_2Si (176 or 182→194), $Pd_{4-x}Te$ (216→227), $PtSn_4$ (41→68), $SrFe_2S_4$ (117→125), $Tb_2(Fe_{0.832}Al_{0.168})_{17}$ (177→191), $Ti_3Al_2N_2$ (159→186), VAu_2 (38→63), V_6C_5 (144→151), VCo_3 LT (187→194), γ-V_4D_3 (27→49), WAl_5 (173→182), δ-Yb_2S_3 (4→11), Zr_4Al_3 (174→191). For all these structures, data conversion is possible without modifying the numerical values of the positional parameters. Reported triclinic $NaSbS_2$ is shown to be identical with $NaSbS_2$ previously refined in space group $C2/c$ and crystallizing with a $KSbS_2$-type structure.

Introduction

One of the problems in comparative crystal chemical studies arises from the number of possible data sets describing the same crystal structure. To make it easier to recognize identical atom arrangements a standardization procedure was developed (Parthé & Gelato, 1984, 1985; Gelato & Parthé, 1987), which selects one single data set within the reported space group. However, for some structures found in the literature, the space group chosen by the authors is incorrect as far as it does not consider all symmetry elements contained in the structure. Since symmetry properties such as polar axes and noncentrosymmetricity are requisites for special physical properties, reporting centrosymmetric structures in noncentrosymmetric space groups for instance, leads the physicist who is looking for materials likely to exhibit particular properties, into error.

In the course of the preparation of a book on inorganic structure types (Parthé, Gelato, Chabot, Penzo & Cenzual, 1991), standardized data sets for some 2000 structure types reported for inorganic compounds (oxides and halides not included) have

* Part II, a complementary list of inorganic structure types with revised space groups, will be submitted to this journal as a Short Communication.

0108-7681/91/040433-07$03.00